# Macrocyclic Complexes of Niobium(III): Synthesis, Structure, and Magnetic Behavior of Mononuclear and Dinuclear Species That Incorporate the $[P_2N_2]$ System

Michael D. Fryzuk,* Christopher M. Kozak, Michael R. Bowdridge, Weichang Jin, Dean Tung, Brian O. Patrick,† and Steven J. Rettig†,‡

*Department of Chemistry, University of British Columbia, 2036 Main Mall, Vancouver, British Columbia, V6T 1Z1 Canada*

*Received May 1, 2001*

The coordination chemistry of the two mixed donor macrocyclic ligands $^{R}[P_2N_2]$ (where $^{R}[P_2N_2] = RP(CH_2SiMe_2NSiMe_2CH_2)_2PR$, R = cyclohexyl (Cy) or phenyl (Ph)) with niobium(III) is presented. The reaction of the dilithio precursors $^{R}[P_2N_2]Li_2(S)$ (R = Cy, S = THF; R = Ph, S = 1,4-dioxane) with $NbCl_3(DME)$ (DME = 1,2-dimethoxyethane) generates the complexes $^{R}[P_2N_2]NbCl$ (R = Cy, **1**; R = Ph, **2**). For R = Cy, single-crystal X-ray diffraction studies and variable-temperature magnetic susceptibility measurements indicate that **1** is mononuclear in the solid state; however, analogous variable-temperature magnetic data suggest that **2** is dinuclear in the solid state due to the observation of antiferromagnetic exchange. In solution, **2** is apparently monomeric similar to **1**. Adduct formation between these mononuclear complexes is also evident; reaction of **2** with neutral donors and coordinating solvents produces the mononuclear derivatives $^{Ph}[P_2N_2]NbCl(L)$ (L = py, CO, $PMe_3$, THF, MeCN), of which the pyridine adduct, **3e**, has been characterized crystallographically. Subsequent replacement of the chlorides can be achieved to generate the paramagnetic alkyl complexes $^{R}[P_2N_2]NbR'$ (R = Cy, Ph; R′ = $CH_2SiMe_3$, $CH(SiMe_3)_2$). The representative compounds $^{Cy}[P_2N_2]NbCH_2SiMe_3$ (**4a**) and $^{Ph}[P_2N_2]NbCH(SiMe_3)_2$ (**5b**) have been characterized by X-ray crystallography.



## Introduction

When complexed to different ancillary ligand sets, niobium can span a wide range of formal oxidation states, from −3 (e.g., $[Nb(CO)_5^{3-}]$) to +5 (e.g., $Cp_2NbH_3$).[1] Depending on the oxidation state, niobium complexes can be used in a variety of purposes; for example, Nb(III) derivatives have been used in stoichiometric organic reactions[2,3] and Nb(V) complexes as arene hydrogenation catalysts.[4−6] While the most common oxidation state of niobium by far is Nb(V),[7] the study of lower oxidation states containing cyclopentadienyl[8−13] and non-cyclopentadienyl[14−19] ancillary ligands is growing. Such low-valent derivatives of niobium have found applications in $N_2$ activation[20−22] and C−N[23−25] bond cleavage processes.

Our approach to developing the chemistry of the early transition elements has been to design multidentate

* E-mail: Fryzuk@chem.ubc.ca.
† Professional Officer: UBC X-ray Structural Chemistry Laboratory.
‡ S.J.R. deceased October 27, 1998.

(1) Cotton, F. A.; Wilkinson, G.; Murillo, C. A.; Bochmann, M. *Advanced Inorganic Chemistry*, 6th ed.; John Wiley and Sons: Toronto, 1999.
(2) Hartung, J. B. J.; Pedersen, S. F. *J. Am. Chem. Soc.* **1989**, *111*, 5468.
(3) Roskamp, E. J.; Pedersen, S. F. *J. Am. Chem. Soc.* **1987**, *109*, 6551.
(4) Rothwell, I. P. *J. Chem. Soc., Chem. Commun.* **1997**, 1331.
(5) Visciglio, V. M.; Clark, J. R.; Nguyen, M. T.; Mulford, D. R.; Fanwick, P. E.; Rothwell, I. P. *J. Am. Chem. Soc.* **1997**, *119*, 3490.
(6) Yu, J. S.; Felter, L.; Potyen, M. C.; Clark, J. R.; Visciglio, V. M.; Fanwick, P. E.; Rothwell, I. P. *Organometallics* **1996**, *15*, 4443.
(7) Wigley, D. E. G., S. D. *Comprehensive Organometallic Chemistry II*; Pergamon: New York, 1995; Vol. 5.
(8) Etkin, N.; Benson, M. T.; Courtenay, S.; McGlinchey, M. J.; Bain, A. D.; Stephan, D. W. *Organometallics* **1997**, *16*, 3504.
(9) Bailey, N. J.; Green, M. L. H.; Leech, M. A.; Saunders: J. F.; Tidswell, H. M. *J. Organomet. Chem.* **1997**, *538*, 111.
(10) Alcalde, M. I.; de la Mata, J.; Gomez, M.; Royo, P.; Pellinghelli, M. A.; Tiripicchio, A. *Organometallics* **1994**, *13*, 462.
(11) de la Mata, J.; Gomez, M.; Gomezsal, P.; Royo, P. *Inorg. Chem.* **1993**, *32*, 5454.
(12) de la Mata, J.; Galakhov, M. V.; Gomez, M.; Royo, P. *Organometallics* **1993**, *12*, 1189.
(13) Gomez, M.; de Ilarduya, J. M. M.; Royo, P. *J. Organomet. Chem.* **1989**, *369*, 197.
(14) Etienne, M.; Carfagna, C.; Lorente, P.; Mathieu, R.; de Montauzon, D. *Organometallics* **1999**, *18*, 3075.
(15) Etienne, M.; Mathieu, R.; Donnadieu, B. *J. Am. Chem. Soc.* **1997**, *119*, 3218.
(16) Lorente, P.; Carfagna, C.; Etienne, M.; Donnadieu, B. *Organometallics* **1996**, *15*, 1090.
(17) Ruppa, K. B. P.; Gambarotta, S.; Yap, G. P. A. *Inorg. Chim. Acta* **1998**, *280*, 143.
(18) Tayebani, M.; Kasani, A.; Feghali, K.; Gambarotta, S.; Bensimon, C. *J. Chem. Soc., Chem. Commun.* **1997**, 2001.
(19) Tayebani, M.; Feghali, K.; Gambarotta, S.; Yap, G. P. A. *Organometallics* **1998**, *17*, 4282.
(20) Berno, P.; Gambarotta, S. *Organometallics* **1995**, *14*, 2159.
(21) Dilworth, J. R.; Henderson, R. A.; Hills, A.; Hughes, D. L.; MacDonald, C.; Stephens, A. N.; Walton, D. R. M. *J. Chem. Soc., Dalton Trans.* **1990**, 1077.
(22) Caselli, A.; Solari, E.; Scopelliti, R.; Floriani, C.; Re, N.; Rizzoli, C.; Chiesi-Villa, A. *J. Am. Chem. Soc.* **2000**, *122*, 3652.
(23) Tayebani, M.; Feghali, H.; Gambarotta, S.; Bensimon, C. *Organometallics* **1997**, *16*, 5084.
(24) Tayebani, M.; Gambarotta, S.; Yap, G. P. A. *Organometallics* **1998**, *17*, 3639.
(25) Kleckley, T. S.; Bennet, J. L.; Wolczanski, P. T.; Lobkovsky, E. B. *J. Am. Chem. Soc.* **1997**, *119*, 247.

10.1021/om010356z CCC: $20.00 
Publication on Web 07/25/2001

**Scheme 1**

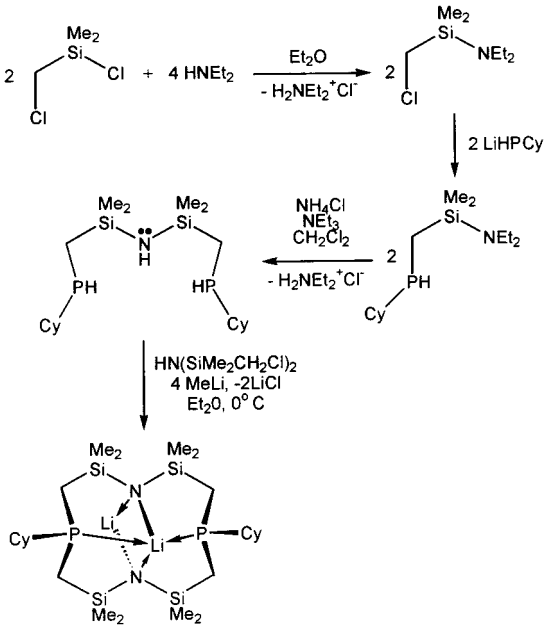


ligands that can support a variety of oxidation states. For example, the combination of amido and phosphine donors in varying ratios has allowed access to a variety of metal complexes in unusual oxidation states, for example, Zr(III) and Hf(III).[26] In this work we examine the characteristic chemistry of Nb(III) complexes that incorporate the $^{R}[P_2N_2]$ macrocyclic ligand, where $^{R}[P_2N_2] = RP(CH_2SiMe_2NSiMe_2CH_2)_2PR$ (R = Cy or Ph).

## Results and Discussion

**Macrocyclic Ligand Synthesis.** We have previously reported the preparation of the *syn*-isomer $^{Ph}[P_2N_2]Li_2$-(THF) by the reaction of $PhPH_2$ with $HN(SiMe_2CH_2Cl)_2$ in the presence of $^{n}$BuLi; this preparation is generally carried out stepwise to first generate $HN(SiMe_2CH_2$-$PPhH)_2$ in virtually quantitative yield followed by a lithium-templated ring closure using 4 equiv of $^{n}$BuLi and an additional 1 equiv of $HN(SiMe_2CH_2Cl)_2$.[27] In diethyl ether, the isolation of $^{Ph}[P_2N_2]Li_2$ proceeds in high yield without the need for high dilution techniques as often found for the synthesis of macrocycles.[28] When we attempted to extend this two-step procedure to cyclohexylphosphine ($CyPH_2$), the initial diphosphine intermediate $HN(SiMe_2CH_2PCyH)_2$ could not be isolated cleanly. Therefore, we examined an alternate procedure based on earlier investigations on the preparation of $HN(SiMe_2CH_2NMe_2)_2$.[29] As shown in Scheme 1, protection of the silicon center by the diethylamido moiety allows formation of $CyPHCH_2SiMe_2NEt_2$, which can be transaminated with $NH_3$ to generate the desired diphosphine $HN(SiMe_2CH_2PCyH)_2$ in excellent yield. Subsequent ring closure in a manner analogous to $^{Ph}[P_2N_2]$ produces the macrocyclic dilithio derivative $^{Cy}[P_2N_2]Li_2$ in acceptable yield as large colorless crystals by low-temperature crystallization from a saturated hexanes solution. The yield can, however, be substantially improved by isolating the less soluble THF adduct $^{Cy}[P_2N_2]Li_2(THF)$ generated by adding a small excess of THF to the hexanes solution and removal of solvents in vacuo. No advantage was found to using the adduct-free ligand; therefore, subsequent metalation reactions employed the use of the THF adduct.

**Scheme 2**

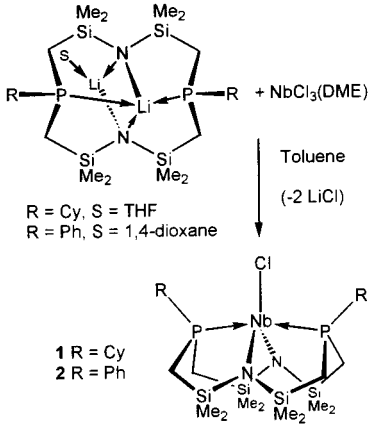


The $^{1}$H NMR spectrum of $^{Cy}[P_2N_2]Li_2(THF)$ is quite similar to the previously reported $^{Ph}[P_2N_2]Li_2(THF)$[27] ligand precursor albeit for the presence of cyclohexyl methylene resonances in lieu of phenyl resonances. The solution structure is consistent with $C_{2v}$ symmetry; only two types of silyl methyl protons are observed in the $^{1}$H NMR spectrum at 0.30 and 0.53 ppm for 12H each. The methylene protons of the macrocycle appear as AB multiplets coupled to phosphorus centered at 0.69 ppm. The resonances of the phosphine cyclohexyl protons appear as broad multiplets at 1.13, 1.60, 1.67, and 1.84 ppm. The resolution of these resonances could not be improved even upon cooling to −80 °C. Two sets of triplet resonances appear for the coordinated THF ligand at 1.27 and 3.57 ppm. In the $^{31}P\{^{1}H\}$ NMR spectrum, the two equivalent phosphorus nuclei give rise to an equal intensity quartet at −32.78 ppm due to coupling to Li. In the $^{7}Li\{^{1}H\}$ NMR spectrum, two resonances are observed—a broadened singlet at 1.22 ppm and a triplet at 2.99 ppm—as a result of coupling to the two aforementioned equivalent $^{31}$P nuclei. This lithium-7 spectrum confirms that this material has the indicated *syn* stereochemistry similar to that found for the phenyl analogue.[27] The *syn* stereochemistry of the THF-free dilithium salt $^{Cy}[P_2N_2]Li_2$ was confirmed unequivocally by single-crystal X-ray structure determination (see Supporting Information).

**Syntheses and Characterization of $^{R}[P_2N_2]NbCl$.** A convenient and versatile starting material for niobium(III) chemistry is $NbCl_3(DME)$ (DME = 1,2-dimethoxyethane).[2,3] Addition of 1 equiv of the ligand precursor $^{R}[P_2N_2]Li_2(S)$ (R = Cy, S = THF; R = Ph, S = 1,4-dioxane) to a suspension of $NbCl_3(DME)$ in toluene results in the slow formation of a dark green solution over 48 h. Upon workup, $^{Cy}[P_2N_2]NbCl$ (**1**) is obtained as green solid, while $^{Ph}[P_2N_2]NbCl$ (**2**) is isolated as a brick red precipitate, both in high yield (Scheme 2). As

(26) Fryzuk, M. D.; Mylvaganum, M.; Zaworotko, M. J.; MacGillivray, L. R. *J. Am. Chem. Soc.* **1993**, *115*, 10360.
(27) Fryzuk, M. D.; Love, J. B.; Rettig, S. J. *J. Chem. Soc., Chem. Commun.* **1996**, 2783.
(28) Lindoy, L. F. *The Chemistry of Macrocyclic Ligand Complexes*; Cambridge University Press: Cambridge, U.K., 1989.
(29) Fryzuk, M. D.; Hoffman, V.; Kickham, J. E.; Rettig, S. J.; Gambarotta, S. *Inorg. Chem.* **1997**, *36*, 3480.

**Table 1. Crystallographic Data**[a]

| | 1 | 3e | 4a | 5b |
|---|---|---|---|---|
| formula | $C_{24}H_{54}N_2P_2Nb_2Si_4Cl\cdot C_6H_{14}$ | $C_{29}H_{47}N_3NbP_2Si_4Cl$ | $C_{28}H_{65}N_2NbP_2Si_5$ | $C_{31}H_{60}N_2NbP_2Si_6$ |
| fw | 759.53 | 740.36 | 725.12 | 784.20 |
| color, habit | green, prism | red, irregular | blue, platelet | green, irregular |
| cryst size, mm | 0.5 × 0.5 × 0.3 | 0.30 × 0.10 × 0.10 | 0.15 × 0.15 × 0.05 | 0.50 × 0.20 × 0.20 |
| cryst syst | orthorhombic | triclinic | monoclinic | monoclinic |
| space group | *Pbcn* (#60) | $P\bar{1}$ (#2) | $P2_1/n$ (#14) | $C2/c$ (#15) |
| *a*, Å | 15.5439(4) | 10.281(3) | 23.139(2) | 20.414(1) |
| *b*, Å | 24.327(1) | 11.435(2) | 16.411(1) | 11.964(1) |
| *c*, Å | 10.8181(3) | 17.230(2) | 22.802(1) | 19.783(2) |
| α, deg | 90 | 84.181(3) | 90 | 90 |
| *β*, deg | 90 | 88.241(3) | 112.770(5) | 119.149(7) |
| *γ*, deg | 90 | 67.291(3) | 90 | 90 |
| *V*, Å$^3$ | 4090.7(2) | 1859.0(5) | 7989.0(9) | 4219.7(7) |
| *Z* | 4 | 2 | 8 | 4 |
| *T*, °C | −100 | −100 | −100 | −100 |
| $\rho_{calc}$, g/cm$^3$ | 1.233 | 1.323 | 1.206 | 1.234 |
| *F*(000) | 1624.00 | 772.00 | 3104.00 | 1660.00 |
| radiation | Mo Kα | Mo Kα | Mo Kα | Mo Kα |
| *μ*, cm$^{-1}$ | 5.76 | 6.33 | 5.51 | 5.54 |
| transmn factors | 0.7058−1.0000 | 0.7477−1.0000 | 0.7290−1.0000 | 0.7742−1.0000 |
| scan type | *ω* | *ω* | *ω* | *ω* |
| scan range, deg in *ω* | 0.5 | 0.5 | 0.5 | 0.5 |
| data collected | full sphere | full sphere | full sphere | full sphere |
| $2\theta_{max}$, deg | 55.7 | 52.9 | 50.2 | 55.8 |
| cryst decay, % | negligible | negligible | negligible | negligible |
| total no. of reflns | 30 918 | 15 166 | 53 102 | 18 053 |
| no. of unique reflns | 4656 | 6715 | 14 340 | 7944 |
| $R_{merge}$ | | 0.051 | 0.119 | 0.042 |
| no. reflns with $I \geq 3\sigma(I)$ | 3871 | 4803 | 6973 | 6381 |
| no. of variables | 182 | 361 | 679 | 213 |
| *R* | 0.050 | 0.071 | 0.087 | 0.06 |
| $R_w$ | 0.090 | 0.118 | 0.155 | 0.092 |
| gof | 1.32 | 1.35 | 1.10 | 1.41 |
| max $\Delta/\sigma$ | 1.41 | 1.16 | 1.76 | 1.39 |
| residual density, e/Å$^3$ | −0.79 | −0.92 | −1.96 | −0.80 |

[a] Rigaku/ADSC CCD diffractometer, $R = \sum||F_o^2| - |F_c^2||/\sum|F_o^2|$; $R_w = (\sum w(|F_o^2| - |F_c^2|)^2/\sum w|F_o^2|^2)^{1/2}$.

will be discussed below, while the solution structures of **1** and **2** are likely mononuclear, the solid state formulations appear to be different.

$^1$H NMR studies for each of **1** and **2** show only broadened resonances from which no structural information could be determined. However, despite the significant line broadening and paramagnetic shift of the resonances, assignments based upon integration and contact shifts could be made that were useful in sample identification and estimation of purity.[30,31] These species are also EPR silent, as would be expected for triplet spin-states.[32] For each complex, mass spectrometry indicates mass/charge fragments corresponding to their respective mononuclear parent peaks, namely, 672 for $^{Cy}[P_2N_2]NbCl$ and 660 for $^{Ph}[P_2N_2]NbCl$. Elemental analyses were also consistent for these formulations. Room-temperature magnetic susceptibility measurements were conducted in solution by Evans' method[33,34] and indicate a magnetic moment of 2.2 $\mu_B$ for **1** and 2.7 $\mu_B$ for **2**, corresponding to two unpaired electrons per niobium and lowered by large spin−orbit couplings in the Nb(III) metal centers.[35]

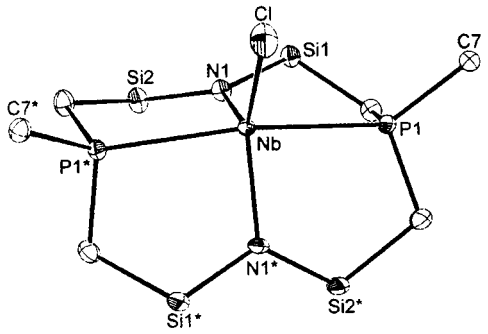


**Figure 1.** Molecular structure (ORTEP) of $^{Cy}[P_2N_2]NbCl$ (**1**). Ellipsoids drawn at the 50% probability level, silyl methyls omitted for clarity, and only *ipso* carbons of cyclohexyl rings shown.

Attempts were made to obtain crystals suitable for X-ray diffraction studies on **1** and **2**. Slow evaporation of a toluene solution of **2** yielded a large crop of dark red prisms, but structure determination was consistently thwarted by crystal twinning. However, green crystals of **1** were obtained from evaporation of a hexanes solution which were suitable for molecular structure determination. The solid state molecular structure of **1** is shown in Figure 1; crystallographic data are shown Table 1, and selected bond lengths and angles in Table 2.

Crystals of **1** contain 0.5 equiv of cocrystallized hexane per $^{Cy}[P_2N_2]NbCl$ molecule. The molecular structure indicates unequivocally that **3** is monomeric in the solid state; it resides on a crystallographic 2-fold axis of

(30) Lamar, G. N.; Horrocks, W. D.; Holm, R. H. *NMR of Paramagnetic Molecules*; Academic Press: New York, 1973.
(31) Drago, R. S. *Physical Methods for Chemists*; 3rd ed.; W. B. Saunders: Orlando, 1996.
(32) Ebsworth, E. A. V.; Rankin, D. W. H.; Craddock, S. *Structural Methods in Inorganic Chemistry*, 2nd ed.; Blackwell Scientific Publications: Oxford, 1991.
(33) Sur, S. K. *J. Magn. Reson.* **1989**, *82*, 169.
(34) Evans, D. F. *J. Chem. Soc.* **1959**, 2003.
(35) Carlin, R. L. *Magnetochemistry*; Springer-Verlag: Heidelberg, 1986.

**Table 2. Selected Bond Lengths (Å) and Angles (deg) in $^{Cy}[P_2N_2]NbCl$, 1**

| | | | |
|---|---|---|---|
| Nb(1)−N(1) | 2.089(1) | Nb(1)−P(1) | 2.5973(4) |
| Nb(1)−Cl(1) | 2.4047(7) | | |
| N(1)−Nb(1)−N(1*) | 112.33(9) | P(1)−Nb(1)−P(1*) | 167.60(2) |
| N(1)−Nb(1)−Cl(1) | 123.84(4) | P(1)−Nb(1)−Cl(1) | 96.20(1) |
| P(1)−Nb(1)−N(1) | 86.92(4) | P(1)−Nb(1)−N(1*) | 86.19(4) |
| Nb(1)−P(1)−C(7) | 130.43(6) | | |
| P(1)−Nb(1)−P(1*)−C(7*) | 166.58(8) | Cl(1)−Nb(1)−P(1)−C(7) | −13.42(8) |

rotation coincident with the molecular $C_2$ symmetry axis defined along the Nb−Cl bond. The niobium center displays a distorted trigonal bipyramidal geometry with the phosphine donors occupying slightly pinched back apical positions giving a P(1)−Nb−P(1*) angle of 167.60(2)°. This angle is larger than the P−M−P angles previously observed in other monomeric early transition metal complexes of the $[P_2N_2]$ ligand.[36,37] The chloride and two amide ligands lie in the trigonal plane, displaying a combined equatorial angle of 360.0°. The Nb−N bond distance of 2.089(1) Å is longer than that reported in $Nb[N(SiMe_3)_2]_2Br_2$,[38] where a Nb−N bond distance of 1.957(4) Å has been found. The Nb−N bonds in **1** are, however, shorter than those found in zirconium and tantalum complexes of $^{Ph}[P_2N_2]$. Both $^{Ph}[P_2N_2]ZrCl_2$[36] and $^{Ph}[P_2N_2]TaMe_3$[37] exhibit M−N lengths averaging 2.1755 Å. It is likely the somewhat longer M−N bonds in the Zr and Ta complexes are because of steric crowding. The Nb−P bond distance of 2.5973(4) Å is similar to that observed in these related monomeric Zr and Ta species, although these complexes contain six- and seven-coordinate $d^0$ metal centers.[37] It is, however, marginally shorter than the Nb−P length in most other reported Nb(III) and Nb(IV) phosphine complexes, where bond lengths on the order of 2.65 Å prevail.[39−44]

**Magnetism Studies of 1 and 2.** Although the structure determination of $^{Cy}[P_2N_2]NbCl$ (**1**) has shown it to be monomeric in the solid state, the solid state structure of $^{Ph}[P_2N_2]NbCl$ (**2**) is still in question. Whereas the color of $^{Cy}[P_2N_2]NbCl$ (**1**) is green in both the solid and solution states, $^{Ph}[P_2N_2]NbCl$ (**2**) is dark red in the solid state but gives dark green solutions in toluene or benzene. One possible explanation is that in the solid state **2** may exist as a chloride-bridged dimer. Similar observations were made for $NbCl_4(PR_3)_2$ complexes.[43,45,46] These dark red or brown solids were found to commonly give green solutions and were strongly solvent dependent. When relatively small phosphines were used ($PMe_3$, $PMe_2Ph$), these species were shown to be dimeric in the solid state and exhibited surprisingly low magnetic moments (0.50 $\mu_{eff}$ for $NbCl_4(PMe_3)_2$), suggesting considerable metal−metal interaction. Variable-temperature solid state magnetic susceptibility measurements

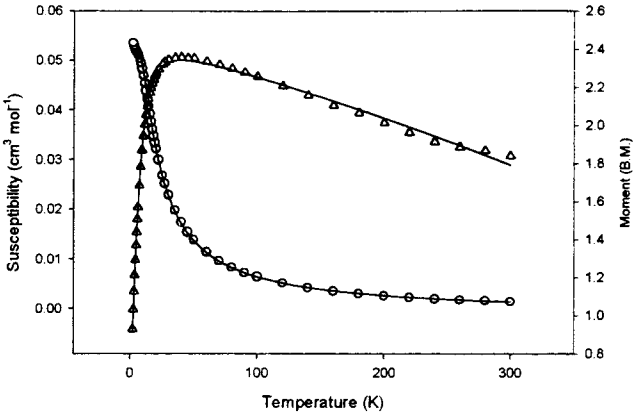


**Figure 2.** Magnetic susceptibility (○) and moment (△) versus temperature plot for $^{Cy}[P_2N_2]NbCl$ (**1**). The zero-field splitting model was employed to generate the lines with $D = 2.03$ cm$^{-1}$, $g = 1.74$, and $P = 0.0068$ ($F = 0.0151$).

on complexes **1** and **2** were conducted to possibly elucidate the nature of the coordination environment around niobium in **2** and to compare the two systems.

The magnetic susceptibility, $\chi_m$, of **1** versus temperature indicates a steady rise in susceptibility at low temperature consistent with a paramagnetic system undergoing no antiferromagnetic exchange. Attempts to model the system using the Curie or Curie−Weiss laws did not provide good fits. Complexes with $S = 1$ spin-states exhibit zero-field splittings that cause deviations from Curie law behavior, particularly those complexes containing second- or third-row transition metals. The magnetic susceptibility data for **1** were therefore analyzed using the equation for the zero-field splitting of a $S = 1$ state:[35]

$$\chi_{Nb} = 1/3\ C\left[\frac{2e^{-x}}{1+2e^{-x}}\right] + 2/3\ C\left[\frac{(2/x)(1-e^{-x})}{1+2e^{-x}}\right] \qquad (1)$$

where $x = D/kT$ and $C = N_A g^2 \mu_B^2/kT$. To account for the presence of a small amount of paramagnetic impurity, the expression was combined with the Curie law term

$$\chi_{para} = \frac{N_A g^2 \mu_B^2 S(S+1)}{3kT} \qquad (2)$$

according to

$$\chi_m = [1-P]\chi_{Nb} + P\chi_{para} \qquad (3)$$

where $P$ represents the fraction of paramagnetic $S = 1$ impurity. Experimental susceptibility versus temperature data for **1** are compared with the best fits from theory (Figure 2) with $D = 2.03$, $g = 1.74$, and $P = 0.0068$ ($F = 0.0151$). The small $g$ value can be rationalized by the large degree of spin−orbit coupling exhibited by second- and third-row metals. This effect is made

(36) Fryzuk, M. D.; Love, J. B.; Rettig, S. J. *Organometallics* **1998**, *17*, 846.
(37) Fryzuk, M. D.; Johnson, S. A.; Rettig, S. J. *Organometallics* **1999**, *18*, 4059.
(38) Bott, S. G.; Hoffman, D. M.; Rangarajan, S. P. *Inorg. Chem.* **1995**, *34*, 4305.
(39) Cotton, F. A.; Lu, J. *Inorg. Chem.* **1995**, *34*, 2639.
(40) Al-Soudani, A.-R. H.; Edwards, P. G.; Hursthouse, M. B.; Malik, K. M. A. *J. Chem Soc., Dalton Trans.* **1995**, 355.
(41) Cotton, F. A.; Roth, W. J. *Inorg. Chim. Acta* **1983**, *71*, 175.
(42) Cotton, F. A.; Roth, W. J. *Inorg. Chem.* **1984**, *22*, 3654.
(43) Cotton, F. A.; Duraj, S. A.; Roth, W. J. *Inorg. Chem.* **1984**, *23*, 3592.
(44) Cotton, F. A.; Roth, W. J. *Polyhedron* **1986**, *4*, 1103.
(45) Manzer, L. E. *Inorg. Chem.* **1977**, *16*, 525.
(46) Labauze, G.; Samuel, E.; Livage, J. *Inorg. Chem.* **1980**, *19*, 1384.

further evident by the plot of magnetic moment versus temperature. At 300 K a magnetic moment of 1.84 $\mu_B$ is observed, significantly lower than the expected spin-only moment of 2.83 $\mu_B$ for two unpaired electrons. As the temperature is lowered, a maximum magnetic moment of 2.34 $\mu_B$ is observed at 40 K. Below 40 K the moment begins to drop more rapidly, since zero-field splitting factors begin to take prominence. In the geometrically distorted trigonal bipyramid the normally degenerate $d_{xz}$ and $d_{yz}$ orbitals may experience variations in energy, resulting in the removal of this degeneracy. In this case, a $d^2$ complex will generate a diamagnetic spin-paired configuration. If the energy difference between the resulting nondegenerate $d_{xz}$ and $d_{yz}$ orbitals is smaller than the spin-pairing energy, a triplet spin-state will result. The low magnetic moment of 1.83 $\mu_B$ at room temperature implies that there exists a thermal equilibrium between the two possible spin states, $S = 1$ and $S = 0$. As the temperature is lowered, the system approaches a pure $S = 1$ spin state with a moment of 2.34 $\mu_B$. This implies a spin-equilibrium where the ground state is the high spin-state. The high−low spin equilibrium case is well documented in the literature,[35,47] but to our knowledge there are no examples of spin equilibrium between $S = 1$ and $S = 0$ Nb(III). A related system displaying a high-spin ground state to low-spin thermally populated state is $FeCl_3(PCy_3)_2$.[48] Variable-temperature magnetic data on this Fe(III) species show a steady increase in magnetic moment with decreasing temperature, indicating a $S = 5/2$ ground state to $S = 3/2$ spin-state transition. Changing the phosphine from $PCy_3$ to $PMe_3$ causes the reverse equilibrium to be observed with a low-spin ground state.

The plot of magnetic susceptibility of the phenyl phosphine-substituted complex **2** versus temperature reveals a broad maximum in susceptibility around 180 K, consistent with the presence of antiferromagnetic coupling. A possible explanation is that species **2** is a chloride-bridged dimer, as previously speculated.[49] The data can be modeled using the Heisenberg model for a $S = 1$ dimer where $C = N_A g^2 \mu_B{}^2/kT$:[35]

$$\chi_m = 2C\left[\frac{e^{2J/kT} + 5e^{6J/kT}}{1 + 3e^{2J/kT} + 5e^{6J/kT}}\right] \quad (4)$$

Paramagnetic impurities in **2** were accounted for as in the analysis of **1** above, albeit using the Curie−Weiss law term, and the data were corrected for temperature-independent paramagnetism (TIP). The best fit between experiment and theory, employing a TIP of $1800 \times 10^{-6}$ $cm^3\ mol^{-1}$ (per dimer unit), shown in Figure 3, yielded $J = -75.74\ cm^{-1}$, $g = 2.11$, $P = 0.0861$, and $\theta = -1.20$ ($F = 0.00918$). Using smaller values of TIP yielded smaller fractions of $P$, but unrealistic $g$ values. It should also be noted that contributions of zero-field splitting and spin−orbit coupling have been omitted to simplify analysis; complicated models employing these factors for magnetically related Ni(II) systems, however, have been examined.[50] Although many reports exist on the magnetic behavior of vanadium-containing species,[51−54] there is little data on low-valent niobium-containing dimers other than those in which Nb−Nb bonds are suggested.[55] Our primary interest lies in the comparison of the magnetic nature of **1** and **2** and the structural differences these data imply. In the absence of a direct crystallographic comparison of the two chloride complexes, the magnetic behavior clearly indicates the structural differences in the solid state.

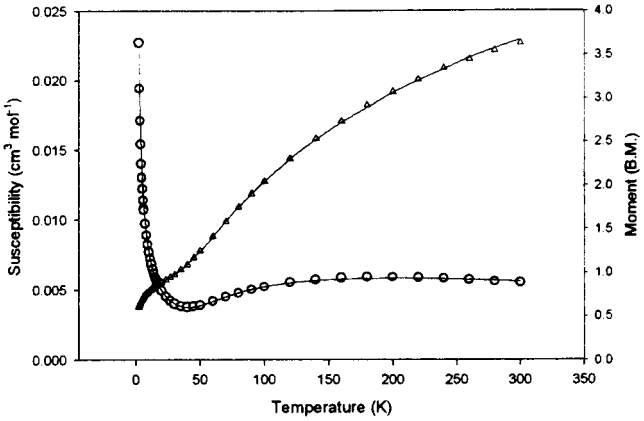


**Figure 3.** Magnetic susceptibility (○) and moment (△) versus temperature plot for $^{Ph}[P_2N_2]NbCl$ (**2**). The $S = 1$ Heisenberg dimer model was employed to generate the lines with $J = -75.74\ cm^{-1}$, $g = 2.11$, $P = 0.0861$, $\theta = -1.20$ K, TIP = $1800 \times 10^{-6}$ $cm^3\ mol^{-1}$ ($F = 0.00918$).

**Adduct Formation Reactions of $^{Ph}[P_2N_2]NbCl$.** Whereas $^{Cy}[P_2N_2]NbCl$ (**1**) is a green solid which dissolves in most hydrocarbon solvents (including hexanes and sparingly in pentane) to give green solutions, red $^{Ph}[P_2N_2]NbCl$ (**2**) is not particularly soluble in hydrocarbon solvents other than aromatics, such as toluene and benzene, in which it gives deep green solutions. Variable-temperature magnetic susceptibility data suggest that complex **2** may be dimeric in the solid state (see above). This color change in solution may imply dissociation of a weakly bound chloride-bridged dimer. In an effort to examine simple adduct formation of **2**, we examined its reactivity with donor ligands; similar reactivity was observed for **1**, but these adducts were characterized only by their UV−visible spectra.

Upon dissolution in THF, **2** generates a yellow solution that corresponds to the formation of the THF adduct $^{Ph}[P_2N_2]NbCl(THF)$ (**3a**). Upon removal of the THF, a brown solid could be obtained, but elemental analysis consistent with the formula of **3a** could not be obtained; furthermore, dissolution of this isolated material in aromatic solvents gave green solutions typical of the starting, adduct-free chloride **2**. A similar set of observations are obtained for the acetonitrile adduct $^{Ph}[P_2N_2]NbCl(NCMe)$ (**3b**). Addition of CO gas to a green benzene-$d_6$ solution of $^{Ph}[P_2N_2]NbCl$ (**2**) quickly yields

(47) Kahn, O. *Molecular Magnetism*; VCH: New York, 1993.
(48) Walker, D.; Poli, R. *Inorg. Chem.* **1989**, *28*, 1793.
(49) Fryzuk, M. D.; Leznoff, D. B.; Rettig, S. J.; Thompson, R. C. *Inorg. Chem.* **1994**, *33*, 5528.
(50) Ginsberg, A. P.; Martin, R. L.; Brookes, R. W.; Sherwood, R. C. *Inorg. Chem.* **1972**, *11*, 2884.
(51) Choukroun, R.; Lorber, C.; Donnadieu, B.; Henner, B.; Frantz, R.; Guerin, C. *J. Chem. Soc., Chem. Commun.* **1999**, 1099.
(52) Choukroun, R.; Donnadieu, B.; Malfant, I.; Haubrich, S.; Frantz, R.; Guerin, C.; Henner, B. *J. Chem. Soc., Chem. Commun.* **1997**, 2315.
(53) Dean, N. S.; Bond, M. R.; O'Conner, C. J.; Carrano, C. J. *Inorg. Chem.* **1996**, *35*, 7643.
(54) Ferguson, R.; Solari, E.; Floriani, C.; Osella, D.; Ravera, M.; Re, N.; Chiesi-Villa, A.; Rizzoli, C. *J. Am. Chem. Soc.* **1997**, *119*, 10104.

**Table 3. UV−Vis Spectral Data and Solution Magnetic Moments for $^{R}[P_2N_2]NbCl(L)$**

| ligand | color | UV−vis (nm) | $\epsilon$ | $\mu_{eff}$ |
|---|---|---|---|---|
| R = Ph | | | | |
| none | green | 616 | 672 | 2.70 |
| THF (**3a**) | yellow | 439 | 997 | 2.69 |
| MeCN (**3b**) | amber | 452 | 1210 | 2.72 |
| CO (**3c**) | bright yellow | 440 | 912 | diamagnetic |
| $PMe_3$ (**3d**) | orange | 425 (shoulder) | 801 | 2.02 |
| py (**3e**) | red | 540 | 1179 | 2.34 |
| R = Cy | | | | |
| none | green | 630 | 614 | |
| THF | lime green | 406 | 458 | |
| MeCN | pale yellow | 427 (shoulder) | 599 | |
| CO | dark yellow | 427 (shoulder) | 601 | |
| $PMe_3$ | bright yellow | 380 (shoulder) | 1036 | |
| py | purple | 549 | 1489 | |

a yellow solution, which reverts to its original green color upon removal of CO under vacuum. The $^1H$ and $^{31}P\{^1H\}$ NMR spectra show the adduct is diamagnetic upon coordination of the strong field ligand CO, the degenerate $d_{xz}$ and $d_{yz}$ orbitals of the trigonal bipyramidal (or square pyramidal) starting material become inequivalent, and the electrons pair. A solution IR measurement shows only one assignable CO stretch at $\nu_{CO}$ = 1920 $cm^{-1}$, consistent with the formulation $^{Ph}[P_2N_2]NbCl(CO)$ (**3c**). This vibration lies within the range observed for other Nb(III) carbonyl derivatives.[12,56−58] Any attempts to isolate a solid product were hindered by the lability of the CO. The addition of $PMe_3$ to a solution of $^{Ph}[P_2N_2]NbCl$ in toluene or cyclohexane also induces a color change from green to orange. The resulting adduct $^{Ph}[P_2N_2]NbCl(PMe_3)$ (**3d**) is paramagnetic, showing only broadened and shifted resonances in the $^1H$ NMR spectrum.

In contrast to the above labile adducts, the addition of pyridine results in the formation of a stable adduct of formula $^{Ph}[P_2N_2]NbCl(py)$ (**3e**). This complex does not dissociate pyridine even under vacuum. NMR spectroscopic measurements indicate that **3e** is paramagnetic, as evidenced by the broadened and shifted resonances observed in the $^1H$ NMR spectrum. Room-temperature solution magnetic susceptibility measurements indicate a magnetic moment of 2.34 $\mu_B$, consistent with two unpaired electrons. Formation of all of the adducts **3a**−**e** can be conveniently followed using UV−visisble spectroscopy (Table 3); all show single isosbestic points upon titration of the starting chloride with the donor ligand. Interestingly, only 1 equiv of pyridine is necessary to complete the formation of **3e**, whereas >10 equiv of donor is necessary for all of the other adducts to form completely. Red single crystals of pyridine adduct **3e** were obtained from a 1:1 toluene−hexanes solution. The solid state X-ray molecular structure of $^{Ph}[P_2N_2]NbCl(py)$ (**3e**) is shown in Figure 4; crystal data are given in Table 1, and selected bond lengths and angles are detailed in Table 4. Structural analysis shows that **3e** is monomeric, with the niobium occupying a distorted octahedral geometry. The equatorial plane is defined by N(1), N(2), N(3), and Cl(1); P(1) and P(2) lie in elongated axial positions. The P(1)−Nb(1)−P(1) bond angle of 164.98(4)° is comparable to that observed in other group 5 $[P_2N_2]$ complexes,[37,59] but slightly smaller than that of **2**. The chloride and pyridine ligands are asymmetrically coordinated to niobium in that the P(1)−Nb(1)−N(3) and P(1)−Nb(1)−Cl(1) angles (92.47° and 92.74°) are smaller than the corresponding P(2)−Nb(1)−N(3) and P(2)−Nb(1)−Cl(1) angles (98.22° and 99.47°). The pyridine ring also adopts a twisted coordination angle with respect to the axis defined by P(1)−Nb(1)−P(2); that is, the P(1)−Nb(1)−N(3)−C(29) torsion angle is 44.6°. This evidently minimizes steric interaction between the pyridine ligand and the chloride while also avoiding close contact with the phenyl rings on $[P_2N_2]$. The phenyl rings themselves are each twisted to different degrees in order to avoid steric congestion caused by interaction with the pyridine. Whereas the phenyl ring bound to P(2) adopts a nearly parallel plane with the P(1)−Nb(1)−P(2) axis, the other phenyl ring approaches a perpendicular orientation. This is demonstrated by the small Nb(1)−P(2)−C(19)−C(20) torsion angle of 7.2° as compared to 70.9° for Nb(1)−P(1)−C(13)−C(18). The Nb−N, −P, and Cl bond lengths are not unusual and compare to other Nb-amido and phosphine complexes including $^{Cy}[P_2N_2]NbCl$, above.[39−44]

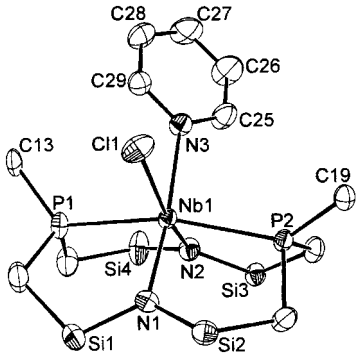


**Figure 4.** Molecular structure (ORTEP) of $^{Ph}[P_2N_2]NbCl(py)$, **3e**. Ellipsoids drawn at the 50% probability level, silyl methyls omitted for clarity, and only *ipso* carbons of phenyl rings shown.

**Scheme 3**

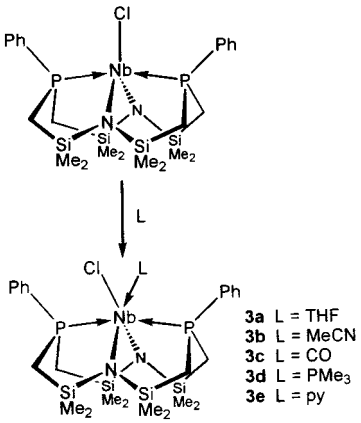


**Reaction of $^{R}[P_2N_2]NbCl$ with $LiCHR'(SiMe_3)$ (R′ = H, $SiMe_3$).** The niobium chloride complexes **1** and **2**



(55) Tayebani, M.; Feghali, K.; Gambarotta, S.; Yap, G. P. A.; Thompson, L. K. *Angew. Chem., Int. Ed.* **1999**, *38*, 3659.
(56) Bunker, M. J.; Green, M. L. H. *J. Organomet. Chem.* **1980**, *192*, C6.
(57) Antinolo, A.; de Ilarduya, J. M.; Otero, A.; Royo, P.; Manotti-Lanfredi, A. M.; Tiripicchio, A. *J. Chem. Soc., Dalton Trans.* **1988**, 2685.
(58) Jalon, F. A.; Otero, A.; Royo, P.; Balcazar, J. L.; Florencio, F. *J. Chem. Soc., Dalton Trans.* **1989**, 79−84.
(59) Fryzuk, M. D.; Johnson, S. A.; Rettig, S. J. *Organometallics* **2000**, *19*, 3931−3941.

**Table 4. Selected Bond Lengths (Å) and Angles (deg) in $^{Ph}[P_2N_2]NbCl(py)$, 3e**

| | | | |
|---|---|---|---|
| Nb(1)−N(1) | 2.125(3) | Nb(1)−P(1) | 2.568(1) |
| Nb(1)−N(2) | 2.152(3) | Nb(1)−P(2) | 2.596(1) |
| Nb(1)−N(3) | 2.398(3) | Nb(1)−Cl(1) | 2.511(1) |
| N(2)−Nb(1)−N(1) | 103.0(1) | P(1)−Nb(1)−P(2) | 164.98(4) |
| N(2)−Nb(1)−Cl(1) | 164.5(1) | Cl(1)−Nb(1)−N(3) | 79.91(9) |
| N(1)−Nb(1)−Cl(1) | 92.2(1) | P(1)−Nb(1)−N(3) | 92.47(9) |
| N(2)−Nb(1)−P(1) | 85.6(1) | P(2)−Nb(1)−N(3) | 98.22(9) |
| N(1)−Nb(1)−P(1) | 85.1(1) | N(1)−Nb(1)−N(3) | 171.7(1) |
| Cl(1)−Nb(1)−P(1) | 92.74(4) | N(2)−Nb(1)−N(3) | 84.7(1) |
| Cl(1)−Nb(1)−P(2) | 99.47(4) | | |
| N(1)−Nb(1)−N(3)−C(29) | −29(1) | Cl(1)−Nb(1)−P(1)−C(13) | 49.9(2) |
| P(1)−Nb(1)−P(2)−C(19) | −166.6(2) | P(2)−Nb(1)−P(1)−C(13) | −165.6(2) |

**Scheme 4**

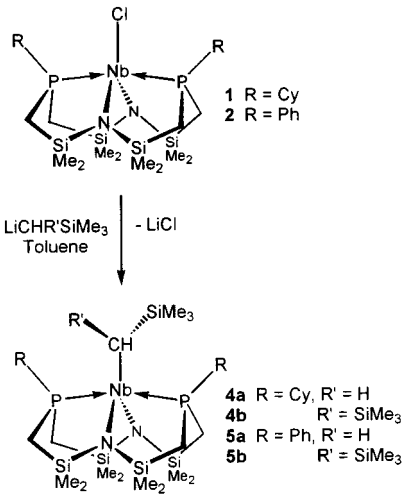


react with bulky alkyllithium reagents to generate stable monomeric niobium alkyl complexes (Scheme 4). Complexes of smaller hydrocarbyl moieties such as methyl can also be synthesized, and this work will be the subject of a future report.[60] The addition of $LiCH_2SiMe_3$ to toluene solutions of **1** and **2** gives dark blue paramagnetic products in each case, whereas the more sterically demanding $LiCH(SiMe_3)_2$ gives green products.

As with the chloride precursors, these complexes show only broadened and shifted resonances in the $^1H$ NMR and no $^{31}P\{^1H\}$ resonances. They are also EPR silent. X-ray crystallography and magnetic studies were, therefore, employed to characterize these $^R[P_2N_2]NbR'$ complexes. Room-temperature magnetic susceptibility measurements were conducted in solution by Evans' method[33,34] and indicate magnetic moments of 2.6 and 2.5 $\mu_B$ for **4a** and **5a**, respectively, corresponding to two unpaired electrons per niobium.

Single crystals of $^{Cy}[P_2N_2]NbCH_2SiMe_3$, **4a**, suitable for X-ray diffraction studies were grown by slow cooling of a saturated hexanes solution. The analogous $^{Ph}[P_2N_2]NbCH_2SiMe_3$, **5a**, exhibits significantly higher solubility in even the most nonpolar solvents such as pentane and hexamethyldisiloxane and could be isolated only as an amorphous solid by drying under high vacuum for several hours. The solid state X-ray molecular structure of **4a** is shown in Figure 5; crystal data are given in Table 1, and selected bond lengths and angles are detailed in Table 5.

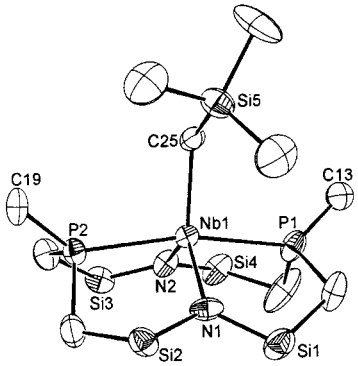


**Figure 5.** Molecular structure (ORTEP) of $^{Cy}[P_2N_2]NbCH_2SiMe_3$, **4a**. Ellipsoids drawn at the 50% probability level, silyl methyls omitted for clarity, and only *ipso* carbons of cyclohexyl rings shown.

**Table 5. Selected Bond Lengths (Å) and Angles (deg) in $^{Cy}[P_2N_2]NbCH_2SiMe_3$, 4a**

| | | | |
|---|---|---|---|
| Nb(1)−N(1) | 2.112(7) | Nb(1)−P(1) | 2.571(3) |
| Nb(1)−N(2) | 2.119(8) | Nb(1)−P(2) | 2.583(2) |
| Nb(1)−C(25) | 2.21(1) | | |
| N(1)−Nb(1)−N(2) | 115.7(3) | P(1)−Nb(1)−P(2) | 166.9(1) |
| N(1)−Nb(1)−C(25) | 123.84(4) | P(1)−Nb(1)−C(25) | 96.20(1) |
| P(1)−Nb(1)−N(1) | 85.7(3) | P(1)−Nb(1)−N(2) | 87.0(2) |
| P(2)−Nb(1)−N(1) | 130.43(6) | P(2)−Nb(1)−N(2) | 85.4(2) |
| Nb(1)−C(25)−Si(5) | 123.3(5) | P(1)−Nb(1)−C(25) | 95.6(3) |
| N(1)−Nb(1)−C(25) | 123.0(3) | | |
| N(1)−Nb(1)−C(25)−Si(5) | 1.8(8) | P(1)−Nb(1)−C(25)−Si(5) | −86.7(6) |

$^{Cy}[P_2N_2]NbCH_2SiMe_3$ crystallizes with two molecules in the asymmetric unit cell. As with the chloride precursor, **1**, the niobium atoms in each asymmetric molecule occupy a distorted trigonal bipyramidal geometry. The phosphine atoms are pinched back from the axial position giving P(1)−Nb(1)−P(2) and P(3)−Nb(2)−P(4) angles of 166.9(1)° and 163.94(9)°, respectively. The alkyl and two amide ligands lie in the trigonal plane, displaying a combined equatorial angle of 360.0° about niobium. The N−Nb−N angles in each asymmetric molecule are quite different, giving a N(1)−Nb(1)−N(2) angle of 115.7(3)° and a N(3)−Nb(2)−N(4) angle of 121.2(3)°. The Nb−N and Nb−P bond lengths are only slightly longer than those exhibited by **1**, indicating that the sterically larger alkyl group does not impose a significant effect upon the macrocycle binding in this case. The Nb−C bond length of 2.21(1) Å and Nb−C−Si bond angle of 123.3(5)° are typical of other niobium (trimethylsilyl)methyl complexes.[15,61−64] The position of

(60) Fryzuk, M. D.; Kozak, C. M.; Patrick, B. O. Manuscript in preparation.

(61) Fu, P.; Khan, M. A.; Nicholas, K. M. *Organometallics* **1992**, *11*, 2607.

(62) Fu, P.; Khan, M. A.; Nicholas, K. M. *Organometallics* **1991**, *10*, 382.

**Table 6. Selected Bond Lengths (Å) and Angles (deg) in $^{Ph}[P_2N_2]NbCH(SiMe_3)_2$, 5b**

| | | | |
|---|---|---|---|
| Nb(1)−N(1) | 2.108(2) | Nb(1)−P(1) | 2.5832(5) |
| Nb(1)−C(13) | 2.270(3) | | |
| N(1)−Nb(1)−N(1*) | 111.36(9) | P(1)−Nb(1)−P(1*) | 167.63(2) |
| N(1)−Nb(1)−C(13) | 123.0(1) | P(1)−Nb(1)−C(13) | 106.13(8) |
| P(1)−Nb(1)−N(1) | 86.06(4) | P(1)−Nb(1)−N(1*) | 86.98(4) |
| Nb(1)−C(13)−Si(3) | 114.1(2) | P(1)−Nb(1)−C(13) | 106.13(8) |
| N(1)−Nb(1)−C(13) | 123.0(1) | P(1*)−Nb(1)−C(13) | 86.24(8) |
| N(1*)−Nb(1)−C(13) | 124.5(1) | | |
| N(1)−Nb(1)−C(13)−Si(3) | −32.7(2) | P(1)−Nb(1)−C(13)−Si(3) | −78.2(2) |

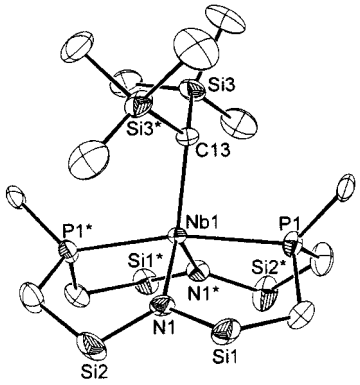


**Figure 6.** Molecular structure (ORTEP) of $^{Ph}[P_2N_2]NbCH(SiMe_3)_2$, **5b**. Ellipsoids drawn at the 50% probability level, silyl methyls omitted for clarity, and only *ipso* carbons of phenyl rings shown.

the $Me_3Si$ fragment of the substituent lies nearly orthogonal to the P−Nb−P axis, as indicated by the P(2)−Nb(1)−C(25)−Si(5) torsion angle of 94.3(6)°. Steric hindrance by the cyclohexyl substituents on the phosphine atoms may force this preferred geometry, resulting in chemically equivalent phosphines. However, in the absence of variable-temperature NMR data, barriers to rotation of the alkyl group about niobium cannot be determined.

The use of the bulkier $CH(SiMe_3)_2$ substituent allows both the cyclohexyl- and phenylphosphine-containing macrocycle complexes to be obtained as crystalline products in high yield. As found for compounds **4a** and **5a** above, $^{R}[P_2N_2]NbCH(SiMe_3)_2$ (R = Cy, **4b**; R = Ph, **5b**) are paramagnetic. Bright green crystals of **4b** and **5b** were obtained by slow evaporation of hexanes solutions. The solid state X-ray molecular structure of **5b** is shown in Figure 6; crystal data are given in Table 1, and selected bond lengths and angles are detailed in Table 6.

The molecule sits on a 2-fold axis of rotation, with C(13) being disordered about this axis. As with **4a**, the niobium atom occupies a trigonal bipyramidal geometry. The P(1)−Nb(1)−P(1*) angle of 167.63(2)° is only marginally larger than that of **4a**, while the N(1)−Nb(1)−N(1*) angle of 111.36(9)° is considerably smaller, possibly as a result of the increased steric bulk of the alkyl group. This is also reflected in the longer Nb(1)−C(13) bond length of 2.270(3) Å. Interestingly, changing the substituent from cyclohexyl to phenyl on the phosphine donor atoms does not alter the niobium−phosphorus bond length significantly. All Nb−P bonds in **4a** and **5b** are approximately 2.58 Å. Also, the relatively similar Nb−P−$C_{ipso}$ angles shown in each complex imply that the coordination geometry is not sensitive to the substituents at phosphorus.

## Conclusions

In this report the synthesis of a cyclohexylphosphine-containing mixed donor macrocycle, $^{Cy}[P_2N_2]$, and its utility in stabilizing Nb(III) complexes are described. The chloride complex $^{Cy}[P_2N_2]NbCl$ (**1**) is monomeric in the solid state, as evidenced by X-ray diffraction and variable-temperature magnetic susceptibility studies. It is a useful precursor to the hydrocarbyl derivatives $^{Cy}[P_2N_2]NbCH_2SiMe_3$ and $^{Cy}[P_2N_2]NbCH(SiMe_3)_2$ by metathesis type procedures. The related complex having phenyl-substituted phosphine donor atoms, $^{Ph}[P_2N_2]NbCl$ (**2**), has also been prepared and studied by variable-temperature magnetic susceptibility measurements. The plot of $\chi_m$ versus temperature indicates the presence of antiferromagnetic exchange between two $d^2$ centers, which is consistent with a dinuclear structure for **2** in the solid state, possibly $(^{Ph}[P_2N_2]Nb)_2(\mu\text{-}Cl)_2$. The Lewis acidic nature of Nb(III) in **2** is evident in its ability to readily form adducts with coordinating solvents and small molecules generating monomeric $^{Ph}[P_2N_2]NbCl(L)$ complexes. As in the cyclohexylphosphine analogue, metathesis of the chloride with alkyllithium reagents generates the monomeric paramagnetic organometallic complexes $^{Ph}[P_2N_2]NbCH_2SiMe_3$ and $^{Ph}[P_2N_2]NbCH(SiMe_3)_2$. Current work is being directed at studying the reactivity patterns exhibited by these Nb(III) alkyl complexes, especially hydrogenolysis and insertion processes.

## Experimental Section

Unless otherwise stated, all manipulations were performed under an atmosphere of dry oxygen-free nitrogen or argon by means of standard Schlenk or glovebox techniques (Vacuum Atmospheres HE-553-2 glovebox equipped with a MO-40-2H purification system and a −40 °C freezer). Hexanes and toluene were purchased anhydrous from Aldrich and further dried by passage through a tower of alumina and degassed by passage through a tower of Q-5 catalyst under positive pressure of nitrogen.[65] Anhydrous diethyl ether and THF were stored over sieves and distilled from sodium benzophenone ketyl under argon. Dichloromethane was dried by refluxing over calcium hydride. Nitrogen and argon were dried and deoxygenated by passing the gases through a column containing molecular sieves and MnO. Deuterated benzene and toluene were dried by refluxing over sodium and potassium alloy, and THF-$d_8$ was dried over sodium, in a sealed vessel

(63) Arnold, J.; Tilley, T. D.; Rheingold, A. L.; Geib, S. J. *Organometallics* **1987**, *6*, 473.

(64) Dorado, I.; Garces, A.; Lopez-Mardomingo, C.; Fajardo, M.; Rodriguez, A.; Antinolo, A.; Otero, A. *J. Chem. Soc., Dalton Trans.* **2000**, 2375.

(65) Pangborn, A. B.; Giardello, M. A.; Grubbs, R. H.; Rosen, R. K.; Timmers, F. J. *Organometallics* **1996**, *15*, 1518.

under partial pressure, and then trap-to-trap distilled. They were degassed under three freeze−pump−thaw cycles. Unless otherwise stated, all NMR spectra were recorded on either a Bruker AC-200 or a Bruker Avance 400 instrument. $^1$H NMR spectra were referenced to residual protons in the deuterated solvent. UV−vis spectra were recorded using a Hewlett-Packard 8454 UV−visible spectrophotometer and quartz cuvettes with Teflon Kontes valves. FTIR spectra were recorded on a BOMEM MB 100 spectrophotometer. Elemental analyses were performed by Mr. P. Borda of this department. Mass spectrometry was performed on a Kratos MS 50 by Mr. M. Lapawa, also of this department. The variable-temperature magnetic susceptibility of powdered samples of **2** and **3** was measured over the range 2−300 K and at a field of 10 000 G using a Quantum Design (MPMS) SQUID magnetometer.

The compounds *syn*-$^{Ph}[P_2N_2]Li_2{\cdot}C_4H_8O_2$,[27] $NbCl_3(DME)$,[3] and $LiCH(SiMe_3)_2$[66] were prepared according to literature procedures. $LiCH_2SiMe_3$ was purchased from Aldrich as a 1 M solution in pentane and used as received. All other reagents were obtained from a commercial source and purified by the appropriate methods.[67] CO gas was purchased from Matheson and used without further purification.

**$ClCH_2SiMe_2NEt_2$.** $HNEt_2$ (25.0 g, 342 mmol) was added to a cooled solution of $Cl(ClCH_2)SiMe_2$ (20.0 g, 140 mmol) in ether at 0 °C and stirred for 2 h before warming to room temperature. Filtration of the flocculent precipitate and removal of solvent under vacuum allowed isolation of a colorless oil. Yield: 21.5 g (85.8%). $^1$H NMR ($C_6D_6$, 200 MHz, 300 K): $\delta$ 0.03 (s, 6H, $SiCH_3$), 0.75 (t, 6H, $CH_2CH_3$), 2.40 (s, 2H, $PCH_2$-Si), 2.50 (q, 4H, $CH_2CH_3$)

**$CyPHCH_2SiMe_2NEt_2$.** *n*-BuLi (75 mL, 1.6 M, 120 mmol) was syringed into a solution of $CyPH_2$ (13.9 g, 120 mol) in $Et_2O$ at −78 °C and allowed to warm to room temperature while stirring. Upon stirring for 1 h at room temperature the yellow solution was transferred to a cooled solution of $ClCH_2SiMe_2$-$NEt_2$ (21.5 g, 120 mmol) in $Et_2O$ at −78 °C. The mixture was allowed to warm to room temperature while stirring. Filtration and removal of solvent allowed isolation of a pale yellow oil. Yield: 28.8 g (92%). $^1$H NMR ($C_6D_6$, 200 MHz, 300 K): $\delta$ 0.03 (s, 6H, $SiCH_3$) 0.30 (m, 2H, $PCH_2Si$), 0.80 (t, 6H, $CH_2CH_3$), 1.1, 1.4, 1.6, 1.8 (br, 11H total, $C_6H_{11}P$), 2.60 (q, 4H, $CH_2CH_3$), 2.80 (ddt, $^1J_{HP}$ = 180 Hz, $^3J_{HH}$ = 20 Hz, $^3J_{HH}$ = 5 Hz $CH_2P$-(*H*)CH). $^{31}P\{^1H\}$ NMR ($C_6D_6$, 81 MHz, 300 K): $\delta$ −60.9 (s).

**$(CyPHCH_2SiMe_2)NH$.** $NH_4Cl$ (6.0 g, 112 mmol), $CyPHCH_2$-$SiMe_2NEt_2$ (28.8 g, 110 mmol), and $CH_2Cl_2$ (100 mL) were cooled to −78 °C. $NEt_3$ (15 mL) was added via syringe, and the mixture was allowed to warm to room temperature and stirred for 18 h. All volatiles were removed in vacuo and the solids extracted into hexanes. Filtration and removal of hexanes allowed isolation of a pale yellow viscous oil. Yield: 17.9 g (83%). $^1$H NMR ($C_6D_6$, 200 MHz, 300 K): 0.10 (s 12H, $SiCH_3$) 0.35 (m, 4H, $PCH_2Si$), 1.1, 1.4, 1.6, 1.8 (br, 22H total, $C_6H_{11}P$), 2.80 (ddt, $^1J_{HP}$ = 180 Hz, $^3J_{HH}$ = 20 Hz, $^3J_{HH}$ = 5 Hz $CH_2P$(*H*)CH). $^{31}P\{^1H\}$ NMR ($C_6D_6$, 81 MHz, 300 K): $\delta$ −60.9 (s).

***syn*-$^{Cy}$[$P_2N_2$]$Li_2$(THF).** $HN(SiMe_2CH_2Cl)_2$ (10.49 g, 45.78 mmol) and $(CyPHCH_2SiMe_2)NH$ (17.90 g, 45.78 mmol) were dissolved in $Et_2O$ (200 mL) and cooled to −78 °C. MeLi (130.8 mL, 1.4 M, 184 mmol) was added, and the solution was allowed to warm to room temperature while stirring, causing a white precipitate to form. After stirring for 12 h all solvents were removed in vacuo and the residue was extracted into toluene and filtered. Evaporation of toluene and washing the crude solids with hexanes allows isolation of a white powder. Crystals suitable for single-crystal X-ray diffraction were grown by cooling a hexanes solution to −40 °C. Yield: 10.9 g (40%).

The yield can be improved by adding 1 equiv of THF to the toluene solution before removal of solvents to generate the less soluble $^{Cy}[P_2N_2]Li_2$(THF) species. Yield: 24.5 g (84%). $^1$H NMR ($C_6D_6$, 400 MHz, 400 K): $\delta$ 0.30 and 0.45 (s, 24H total, $SiCH_3$), 0.57 and 0.85 (m, 8H total, ring $CH_2$), 1.12, 1.60, 1.67, and 1.83 (br, 22H total, $C_6H_{11}P$), 1.27 (m, 4H, THF-$OCH_2CH_2$), 3.57 (m, 4H, THF-$OCH_2CH_2$). $^{31}P\{^1H\}$ NMR ($C_6D_6$, 162 MHz, 300 K): $\delta$ −32.78 (q, $^1J_{PLi}$ = 52.1 Hz). $^7Li\{^1H\}$ ($C_6D_6$, 155.5 MHz, 300 K): $\delta$ 1.22 (s, 1Li), 2.99 (t, $^1J_{LiP}$ = 52.1 Hz, 1Li). Anal. Calcd for $C_{24}H_{54}N_2Si_4P_2Li_2$: C, 52.58; H, 9.74; N, 5.01. Found: C, 51.84; H, 9.79; N, 4.90.

**$^{Cy}$[$P_2N_2$]NbCl (1).** A mixture of $^{Cy}[P_2N_2]Li_2$(THF) (7.00 g, 10.4 mmol) and $NbCl_3$(DME) (3.00 g, 10.4 mmol) was suspended in 100 mL of toluene. After stirring the red suspension for 2 days a dark green solution formed. The solution was evaporated to dryness, extracted into toluene, and filtered through Celite. The toluene was removed in vacuo to produce a dark green powder, which was washed in minimal hexanes and recrystallized from slow cooling of a saturated toluene solution, giving **2** as large dark green prisms. Yield: 5.17 g (75%). $^1$H NMR ($C_6D_6$, 400 MHz, 300 K): $\delta$ 4.78 ($w_{1/2}$ 84 Hz, 12H, $SiCH_3CH_3'$); 11.19 (208 Hz, 12H, $SiCH_3CH_3'$); 11.95 (140 Hz, 4H, *o*-Ph); 39.65 (856 Hz, 4H, PC*H*H′) 56.16 (1244 Hz, 4H, PCH*H*′). UV−vis ($C_6H_{12}$): 620 nm, $\epsilon$ = 712. Anal. Calcd for $C_{24}H_{54}ClN_2NbP_2Si_4$: C, 42.81; H, 8.08; N, 4.16. Found: C, 43.01; H, 8.23; N, 4.30. MS (EI) *m*/*z* (%): 672, (60) [$M^+$]. $\mu_{eff}$ (Evans' method) = 2.20 $\mu_B$.

**$^{Ph}$[$P_2N_2$]NbCl (2).** A mixture of $^{Ph}[P_2N_2]Li_2$(dioxane) (6.65 g, 10.4 mmol) and $NbCl_3$(DME) (3.00 g, 10.4 mmol) was suspended in 100 mL of toluene. After stirring the red suspension for 2 days a dark green solution formed. The solution was evaporated to dryness, extracted into toluene, and filtered through Celite. The toluene was removed in vacuo to produce a brick red powder, which was washed in minimal hexanes and recrystallized from slow cooling of a saturated toluene solution, giving **3** as dark red cubes. Yield: 5.50 g (80%). $^1$H NMR ($C_6D_6$, 400 MHz, 300 K): $\delta$ 4.78 ($w_{1/2}$ 84 Hz, 12H, $SiCH_3CH_3$), 8.70 (28 Hz, 2H, *p*-Ph), 10.22 (48 Hz, 4H, *m*-Ph), 11.19 (208 Hz, 12H, $SiCH_3CH_3$), 11.95 (140 Hz, 4H, *o*-Ph), 39.65 (856 Hz, 4H, PC*H*H), 56.16 (1244 Hz, 4H, PCH*H*′). UV−vis ($C_6H_{12}$): 616 nm, $\epsilon$ = 672. Anal. Calcd for $C_{24}H_{42}ClN_2$-$NbP_2Si_4$: C, 43.59; H, 6.04; N, 4.24; Cl, 5.36. Found: C, 43.34; H, 6.32; N, 4.19; Cl, 5.49. MS (EI) *m*/*z* (%): 660, (70) [$M^+$]. $\mu_{eff}$ (Evans' method) = 2.70; (magnetic susceptibility balance) = 2.80 $\mu_B$.

**Reactions with Coordinating Ligands.** Identical procedures were used for the reaction of $^{Ph}[P_2N_2]$NbCl and $^{Cy}[P_2N_2]$-NbCl with coordinating ligands. Experimental details and characterization of only the $^{Ph}[P_2N_2]$NbCl(L) complexes are described.

**$^{Ph}$[$P_2N_2$]NbCl(THF) (3a).** $^{Ph}[P_2N_2]$NbCl (200 mg, 0.303 mmol) was dissolved in THF (15 mL), giving a deep yellow-colored solution. The solution was stirred for 30 min before all volatiles were removed in vacuo, allowing isolation of a dark yellow solid. The THF molecule is considerably labile, and attempts to dissolve the product in toluene and benzene caused its displacement and regeneration of $^{Ph}[P_2N_2]$NbCl. Yield: 220 mg (99%). $^1$H NMR only partially assignable (THF-$d_8$, 400 MHz, 300 K): $\delta$ 4.20 ($w_{1/2}$ 56 Hz, 12H, $SiCH_3CH_3$), 5.96 (72 Hz, 12H, $SiCH_3CH_3$), 8.85 (22 Hz, 2H, *p*-Ph), 10.80 (46 Hz, 4H, *m*-Ph). UV−vis ($C_6H_{12}$/THF): 439 nm, $\epsilon$ = 997. $\mu_{eff}$ (Evans' method) = 2.69 $\mu_B$.

**$^{Ph}$[$P_2N_2$]NbCl($CH_3CN$) (3b).** $^{Ph}[P_2N_2]$NbCl (200 mg, 0.303 mmol) was dissolved in acetonitrile (15 mL), giving a deep yellow solution. The solution was stirred for 30 min before all volatiles were removed in vacuo, allowing isolation of a dark yellow-brown waxy solid. Dissolution in hexanes or toluene caused slow product decomposition to $^{Ph}[P_2N_2]$NbCl. [$P_2N_2$]-NbCl(NCMe) Yield: 210 mg (99%). UV−vis ($C_6H_{12}$/MeCN): 452 nm, $\epsilon$ = 1210. $\mu_{eff}$ (Evans' method) = 2.72 $\mu_B$.

(66) Cowley, A. H.; Kemp, R. A. *Synth. React. Inorg. Met.-Org. Chem.* **1981**, *11*, 591.

(67) Perrin, D. D.; Armarego, W. L. F. *Purification of Laboratory Chemicals*, 3 ed.; Butterworth-Heinemann Ltd.: Oxford, 1994.

**$^{Ph}$[$P_2N_2$]NbCl(CO) (3c).** A solution of $^{Ph}$[$P_2N_2$]NbCl (10 mg) in $C_6D_6$ was loaded into an NMR tube fitted with a Teflon tap and degassed by three freeze−pump−thaw cycles. The sample was then subjected to 1 atm of CO and sealed. The CO ligand is highly labile and is readily removed under vacuum. $^1$H NMR ($C_6D_6$, 400 MHz, 300 K): $\delta$ 0.24 (br, 24H total SiC$H_3$), 1.74 (br, 8H, PC$H_2$), 7.23, 8.18 (br, PPh). $^{31}$P{$^1$H} NMR ($C_6D_6$, 162 MHz, 300 K): $\delta$ 10.70 ($w_{1/2}$ 852.5 Hz). IR $\nu_{CO}$ 1920 cm$^{-1}$. UV−vis ($C_6H_{12}$): 440 nm, $\epsilon$ = 912.

**$^{Ph}$[$P_2N_2$]NbCl($PMe_3$) (3d).** A solution of $^{Ph}$[$P_2N_2$]NbCl (10 mg) in $C_6D_6$ was loaded into an NMR tube fitted with a Teflon tap and degassed by three freeze−pump−thaw cycles. The sample was then subjected to an excess of $PMe_3$ added by vacuum transfer and sealed. Upon warming to room temperature, the solution turned from an intense green color to dark yellow-orange. The $PMe_3$ ligand is labile and is easily removed under vacuum. $^1$H NMR ($C_6D_6$, 400 MHz, 300 K): $\delta$ 3.78 ($w_{1/2}$ 172 Hz, 12H, SiC$H_3$CH$_3$′); 8.82 (22 Hz, 2H, *p*-Ph); 9.61 (36 Hz, 4H, *m*-Ph); 10.38 (132 Hz, 12H, SiCH$_3$C$H_3$′). UV−vis ($C_7H_8$): 425 nm, $\epsilon$ = 801. $\mu_{eff}$ (Evans' method) = 2.02 $\mu_B$.

**$^{Ph}$[$P_2N_2$]NbCl(py) (3e).** $^{Ph}$[$P_2N_2$]NbCl (200 mg, 0.303 mmol) was dissolved in pyridine (15 mL), giving a deep red solution. The solution was stirred for 30 min before all volatiles were removed in vacuo, allowing isolation of a blood red solid. Slow cooling to −35 °C of a saturated 50:50 toluene/hexanes solution produced a crop of bright red prisms. Yield: 180 mg (80%). $^1$H NMR, only partially assignable ($C_6D_6$, 400 MHz, 300 K): $\delta$ −35.61 ($w_{1/2}$ 828 Hz) −20.56 (1008 Hz) 4.03 (63 Hz, 12H, SiC$H_3$CH$_3$) 6.13 (63 Hz,12H, SiCH$_3$C$H_3$) 8.37 (18 Hz) 10.63 (48 Hz) 11.96 (288 Hz) 15.24 (57 Hz) 39.30 (1011 Hz). UV−vis ($C_6H_{12}$): 540 nm, $\epsilon$ = 1179. $\mu_{eff}$ (Evans' method) = 2.34 $\mu_B$. Anal. Calcd for $C_{29}H_{47}N_3NbP_2Si_4$: C, 47.05; H, 6.67; N, 4.97. Found: C, 47.25; H, 6.76; N, 4.86. MS (EI) *m*/*z* (%): 739, (10) [M]$^+$, 660, (80) [M$^+$ − py].

**Synthesis of Paramagnetic Niobium Alkyl Complexes.**

**$^{Cy}$[$P_2N_2$]NbC$H_2$SiMe$_3$ (4a).** $^{Cy}$[$P_2N_2$]NbCl (3.00 g, 4.46 mmol) and LiC$H_2$SiMe$_3$ (420 mg, 4.46 mmol) were dissolved in toluene (50 mL) and stirred for 12 h to give a bright indigo solution. Solvents were removed in vacuo, resulting in a dark blue residue that was extracted into hexanes and filtered through Celite. Removal of hexanes afforded an indigo-colored solid that was washed with hexamethyldisiloxane to give an analytically pure product. X-ray quality crystals of the paramagnetic product were obtained by extracting the solids into minimal hexamethyldisiloxane and slowly evaporating the solvent over a period of weeks. Yield: 3.00 g (95%). $^1$H NMR only partially assignable ($C_6D_6$, 400 MHz, 300 K): $\delta$ 4.74 ($w_{1/2}$ 76 Hz, 12H, SiC$H_3$CH$_3$), 7.55 (120 Hz, 9H, Si(C$H_3$)$_3$), 10.49 (108 Hz, 12H, SiCH$_3$C$H_3$), 48.61 (748 Hz, 4H, PC*H*H), 85.02 Hz, 4H, PCH*H*). Anal. Calcd for $C_{28}H_{65}N_2NbP_2Si_5$: C, 46.38; H, 9.04; N, 3.86. Found: C, 46.18; H, 9.12; N, 3.79. MS (EI) *m*/*z* (%): 724, (20) [M$^+$]. $\mu_{eff}$ (Evans' method) = 2.6 $\mu_B$.

**$^{Ph}$[$P_2N_2$]NbC$H_2$SiMe$_3$ (5a).** To a solution of $^{Ph}$[$P_2N_2$]NbCl (2.48 g, 3.76 mmol) in toluene (30 mL) was added LiC$H_2$SiMe$_3$ (350 mg, 3.76 mmol) at room temperature. A color change from dark green to dark blue was observed within moments. After stirring for 12 h the solution was filtered through Celite and the solvent removed in vacuo to yield a waxy blue-green solid that was washed with minimal pentane. Yield: 2.50 g (95%). $^1$H NMR ($C_6D_6$, 400 MHz, 300 K): $\delta$ 4.74 ($w_{1/2}$ 76 Hz, 12H, SiC$H_3$CH$_3$), 7.55 (120 Hz, 9H, Si(C$H_3$)$_3$), 8.91 (24 Hz, 2H, *p*-Ph), 10.49 (108 Hz, 12H, SiCH$_3$C$H_3$), 10.81 (52 Hz, 4H, *m*-Ph), 13.77 (288 Hz, 4H, *o*-Ph), 48.61 (748 Hz, 4H, PC*H*H), 85.02 Hz, 4H, PCH*H*). Anal. Calcd for $C_{28}H_{53}N_2NbP_2Si_5$: C, 47.17; H, 7.49; N, 3.93. Found: C, 46.79; H, 7.29; N, 3.99. MS (EI) *m*/*z*, (%): 712, (60) [M$^+$]. $\mu_{eff}$ (Evans' method) = 2.5 $\mu_B$.

**$^{Cy}$[$P_2N_2$]NbCH(SiMe$_3$)$_2$ (4b).** To a solution of $^{Cy}$[$P_2N_2$]NbCl (1.00 g, 1.49 mmol) in toluene (30 mL) was added LiCH(SiMe$_3$)$_2$ (250 mg, 1.50 mmol) at room temperature to give a dark green solution. After stirring for 6 h the solution was filtered through Celite and the solvent removed in vacuo to leave a green solid, which was washed with minimal pentane. Yield: 1.18 g (90%). $^1$H NMR only partially assignable ($C_6D_6$, 400 MHz, 300 K): $\delta$ 4.50 ($w_{1/2}$ 90 Hz, 6H, SiC$H_3$CH$_3$), 5.20 (90 Hz, 6H, SiC$H_3$CH$_3$), 7.70 (500 Hz, 18H, Si(C$H_3$)$_3$), 8.60 (90 Hz, 6H, SiCH′$_3$C$H$′$_3$), 10.20 (90 Hz, 6H, SiC$H$′$_3$CH′$_3$), 13.80 (500 Hz, 2H, PC*H*H) 21.00 (500 Hz, 2H PCH*H*). Anal. Calcd for $C_{31}H_{73}N_2NbP_2Si_6$: C, 46.70; H, 9.23; N, 3.51. Found: C, 46.74; H, 9.28; N, 3.32. MS (EI) *m*/*z* (%): 796, (30) [M$^+$]. $\mu_{eff}$ (Evans' method) = 2.6 $\mu_B$.

**$^{Ph}$[$P_2N_2$]NbCH(SiMe$_3$)$_2$ (5b).** (a) To a solution of $^{Ph}$[$P_2N_2$]-NbCl (1.00 g, 1.51 mmol) in toluene (30 mL) was added LiCH-(SiMe$_3$)$_2$ (250 mg, 1.51 mmol) at room temperature to give a dark green solution. After stirring for 6 h the solution was filtered through Celite and the solvent removed in vacuo to yield green solids, which were washed with minimal pentane. Yield: 1.18 g (90%). $^1$H NMR ($C_6D_6$, 400 MHz, 300 K): $\delta$ 4.35 ($w_{1/2}$ 90 Hz, 6H, SiC$H_3$CH$_3$), 5.20 (90 Hz, 6H, SiC$H_3$CH$_3$), 7.70 (500 Hz, 18H, Si(C$H_3$)$_3$), 8.60 (90 Hz, 6H, SiCH′$_3$C$H$′$_3$), 9.20 (28 Hz, 2H, *p*-Ph), 10.20 (90 Hz, 6H, SiC$H$′$_3$CH′$_3$), 10.80, 11.20 (24 Hz, 36 Hz, 8H total, *o*, *m*-Ph), 13.80 (500 Hz, 2H, PC*H*H) 21.00 (500 Hz, 2H PCH*H*). Anal. Calcd for $C_{31}H_{61}N_2NbP_2Si_6$: C, 47.42; H, 7.83; N, 3.57. Found: C, 47.29; H, 7.75; N, 3.43. MS (EI) *m*/*z* (%): 784, (80) [M$^+$]. $\mu_{eff}$ (Evans' method) = 2.6 $\mu_B$.

**X-ray Crystallographic Analyses of 1, 3a, 4a, and 5b.** In all cases, suitable crystals were selected and mounted on a glass fiber using Paratone-N crystal mounting oil and freezing to −100 °C. All measurements were made on a Rigaku/ADSC CCD area detector with graphite-monochromated Mo K$\alpha$ radiation. Crystallographic data appear in Table 1. In each case the data were processed[68] and corrected for Lorentz and polarization effects and absorption. Neutral atom scattering factors for all non-hydrogen atoms were taken from the *International Tables for X-ray Crystallography*.[69,70] All structures were solved by direct methods[71] and expanded using Fourier techniques.[72] All non-hydrogen atoms were refined anisotropically. Hydrogen atoms were included but not refined. Hydrogen atoms were fixed in calculated positions with C−H = 0.98 Å.

**Acknowledgment.** Professor Robert C. Thompson and Victor Sanchez (UBC) and Professor Natia L. Frank (University of Washington) are gratefully thanked for help in measurement of the magnetic susceptibilities of **1** and **2**, respectively, and for stimulating discussions on the subject of magnetism. We thank both the NSERC of Canada and the Petroleum Research Fund administered by the American Chemical Society for generous financial support.

**Supporting Information Available:** Complete crystallographic data including ORTEP diagrams, bond lengths and angles, final atomic coordinates and equivalent isotropic thermal parameters, anisotropic thermal parameters, intermolecular contacts, and least squares planes are available for complexes **1**, **3e**, **4a**, **5b**, and $^{Cy}$[$P_2N_2$]Li$_2$. This material is available free of charge via the Internet at http://pubs.acs.org.

OM010356Z

(68) teXsan *Crystal Structure Analysis Package*; Molecular Structure Corp.: The Woodlands, TX, 1995.
(69) *International Tables for X-Ray Crystallography*; Kluwer Academic: Boston, MA, 1992; Vol. C, pp 200−206.
(70) *International Tables for X-Ray Crystallography*; Kynoch Press: Birmingham, U.K. (present distributer Kluwer Academic: Boston, MA), 1974; Vol. IV, pp 99−102.
(71) Altomare, A.; Burla, M. C.; Cammali, G.; Cascarano, M.; Giacovazzo, C.; Guagliardi, A.; Moliterni, A. G. G.; Polidori, G.; Spagna, A. *SIR97: A new tool for crystal structure determination and refinement*; 1999.
(72) Beurskens, P. T.; Admiraal, G.; Beurskens, G.; Bosman, W. P.; de Gelder, R.; Israel, R.; Smits, J. M. M. *DIRDIF94; The DIRDIF-94 program system, Technical Report of the Crystallography Laboratory*; University of Nijmegen: The Netherlands, 1994.